Lab on a Chip

Supplementary Information for: Nanofluidic-based Electrochemical Pump for Remotely Controlled, On-Demand Drug Delivery

Marco M. Paci,[1,2], Nicola Di Trani,[1], Paolo Bolla,[1,3], Fabiana Del Bono,[1,3], Takuma Yoshikawa,[4,5], Isaac Tichy,[1,6], Patrick S. Stayton,[4,5], Alessandro Grattoni,[1,7,8]*

[1]Department of Nanomedicine, Houston Methodist Research Institute, Houston, TX 77030, USA;

[2]Medical School, Swansea University, Swansea, SA2 8QA, UK;
[3]Department of Applied Science and Technology, Politecnico di Torino, Torino, 10129, Italy;
[4]Department of Bioengineering, University of Washington, Seattle, WA 98195, USA
[5]Department of Molecular Engineering & Sciences Institute, University of Washington, Seattle, WA 98105, USA;
[6]College of Engineering, University of Florida, Gainesville, FL 32603, USA;
[7]Department of Surgery, Houston Methodist Research Institute, Houston, TX 77030, USA;
[8]Department of Radiation Oncology, Houston Methodist Research Institute, Houston, TX 77030, USA.

*Correspondence: agrattoni@houstonmethodist.org (A.G.); Tel.: +1-(713)-441-7324 (A.G.)

Supplementary note 1: *Drug molecule stability under electrochemical actuation*

To evaluate the potential risk of drug degradation during electrochemical operation, UV–Vis spectroscopy was performed on drug solutions subjected to multiple actuation cycles (0-50 cycles) under the same conditions employed for in vitro modulated release. Each cycle consisted of an ON phase (–2 VDC applied for 1 h) followed by an OFF phase (open-circuit potential for 2 h). Vitamin B12 (VitB12, 600 µg mL^{-1} in PBS) and poly(styrene sulfonate) (PSS, 1 mg mL^{-1} in PBS) were tested. Prior to analysis, samples were diluted 1:50 to fall within the absorbance range of the spectrophotometer. The resulting spectra revealed no measurable changes in absorbance intensity or spectral peak position after repeated electrochemical cycling (Fig. S1A–B). Complementary FTIR spectra were collected on samples before cycling and after 50 cycles to assess chemical integrity in the mid-IR. Spectra were acquired in ATR mode (diamond crystal) with a DTGS-KBr detector (64 scans per spectrum, 0.5 cm^{-1} resolution, 4000–525 cm^{-1} range); a fresh background was collected before each sample. For each condition, 100 µL of sample solution was deposited onto 100 mg of spectroscopic-grade KBr powder, dried under vacuum overnight to remove residual water, and subsequently pressed into a transparent KBr pellet. For VitB12, diagnostic bands remained at the same positions before and after electrochemical actuation: broad N–H/O–H stretch (~3300–3500 cm^{-1}), Amide I (ν C=O, ~1655 cm^{-1}), Amide II (δ N–H + ν C–N, ~1540 cm^{-1}), and C–N/C–O modes in the fingerprint region (~1150 cm^{-1}) (Fig. S1C). For PSS, the spectra preserved the aromatic C=C band (~1600 cm^{-1}) and the sulfonate stretches—$\nu_{as}(SO_3^-)$ (~1195 cm^{-1}) and $\nu_s(SO_3^-)$/S=O (~1030 cm^{-1})—with unchanged positions (Fig. S1D). No new bands were detected and no systematic peak shifts (>5–10 cm^{-1}) were observed. Minor baseline/intensity

differences are consistent with pathlength/loading variation rather than chemistry. UV–Vis and FTIR results indicate preservation of the molecular structure of the analytes, with no detectable formation of new species under the applied actuation conditions. From a mechanistic perspective, these findings suggest that the electrolysis-driven pressure actuation is confined to water electrolysis at the electrode surfaces, without inducing secondary chemical reactions that alter drug stability—an important requirement for translational use.

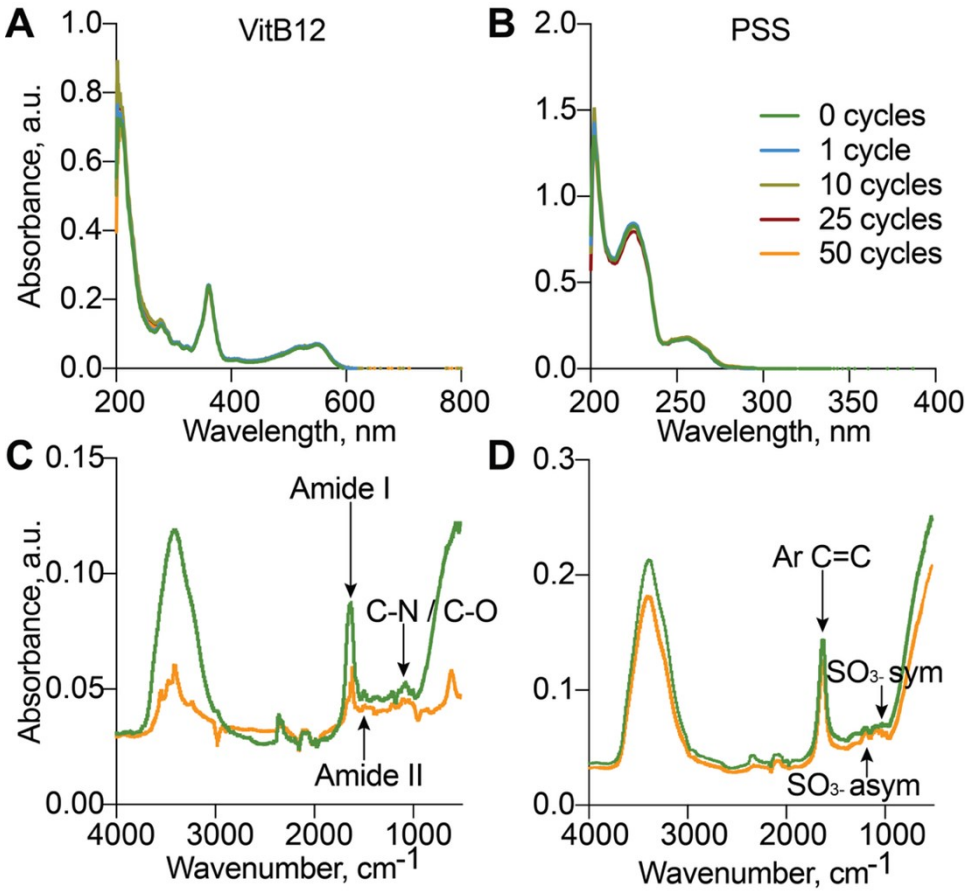

Figure S1. Drug molecule stability under electrolysis cycles. (A-B) UV–Vis spectra of (A) VitB12 and (B) PSS measured after increasing numbers of electrolysis cycles (0-50 cycles). (C–D) FTIR spectra acquired before and after 50 actuation cycles for (C) VitB12 and (D) PSS.

Supplementary note 2: *Electrochemical stability and long-term performance limitations*

Cyclic voltammetry (CV) measurements were performed over an 8-week period on nanofluidic membrane samples stored at 37 °C to simulate physiological conditions and assess long-term electrochemical performance. As shown in *Fig. S2*, a gradual decrease in current response was observed over time, suggesting a decline in catalytic activity and indicating progressive electrochemical degradation of the membrane. This trend highlights a potential limitation of the actuator: the reduced electrochemical efficiency could impair the system's ability to generate sufficient pressure for drug delivery over extended durations. Such degradation may ultimately

impact long-term stability and actuation reliability *in vivo*. Future work will focus on improving electrode durability through advanced fabrication methods and material optimization to support long-term use in physiological environments.

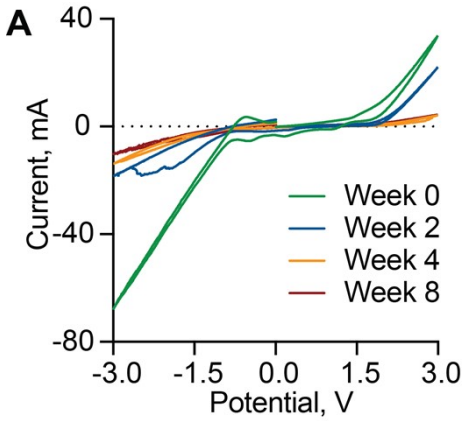

Figure S2. Electrochemical degradation of the nanofluidic membrane. (A) Cyclic voltammetry (CV) profiles of nanofluidic membranes stored at 37 °C, simulating physiological degradation conditions, to assess catalytic efficiency and long-term electrochemical stability.

Supplementary note 3: *Visual demonstration of electrochemical pump working principle*

A custom-made dual-reservoir setup was designed to directly visualize the actuation of the nanofluidic-based electrochemical pump. The system was assembled in a manner similar to the in vitro drug release experiments, but here the top portion of the device was sealed with a transparent glass slide to enable real-time optical imaging of bubble formation and drug transport (Fig. S3A). VitB12 was used as the model compound due to its strong visible absorption, which facilitates colorimetric tracking. The color change in the sink reservoir was analysed using Python-based image processing. A region of interest (ROI) was defined within the sink reservoir, and the normalized red intensity was calculated as the red channel intensity divided by the sum of all three RGB channels. This normalization compensates for fluctuations in illumination or camera exposure, thereby providing a robust metric that reflects relative changes in red coloration due to drug transport, while minimizing noise from external lighting variations (Fig. S3B). The recorded frames show that during electrochemical actuation (–2 VDC applied between the Pt-sputtered nanofluidic membrane electrode and the Pt mesh counter electrode), the drug reservoir becomes partially filled with gas bubbles, consistent with pressure measurements reported in the main text. Under this condition, VitB12 is actively transported into the sink reservoir, which gradually turns red. Importantly, upon termination of the actuation (open-circuit potential), bubble formation ceases and drug release returns to baseline levels (Fig. S3C). Over longer timescales, the generated bubbles slowly dissolve back into the solution as gases re-equilibrate with their solubility limits, consistent with diffusion-limited bubble dissolution phenomena described in confined electrochemical systems.

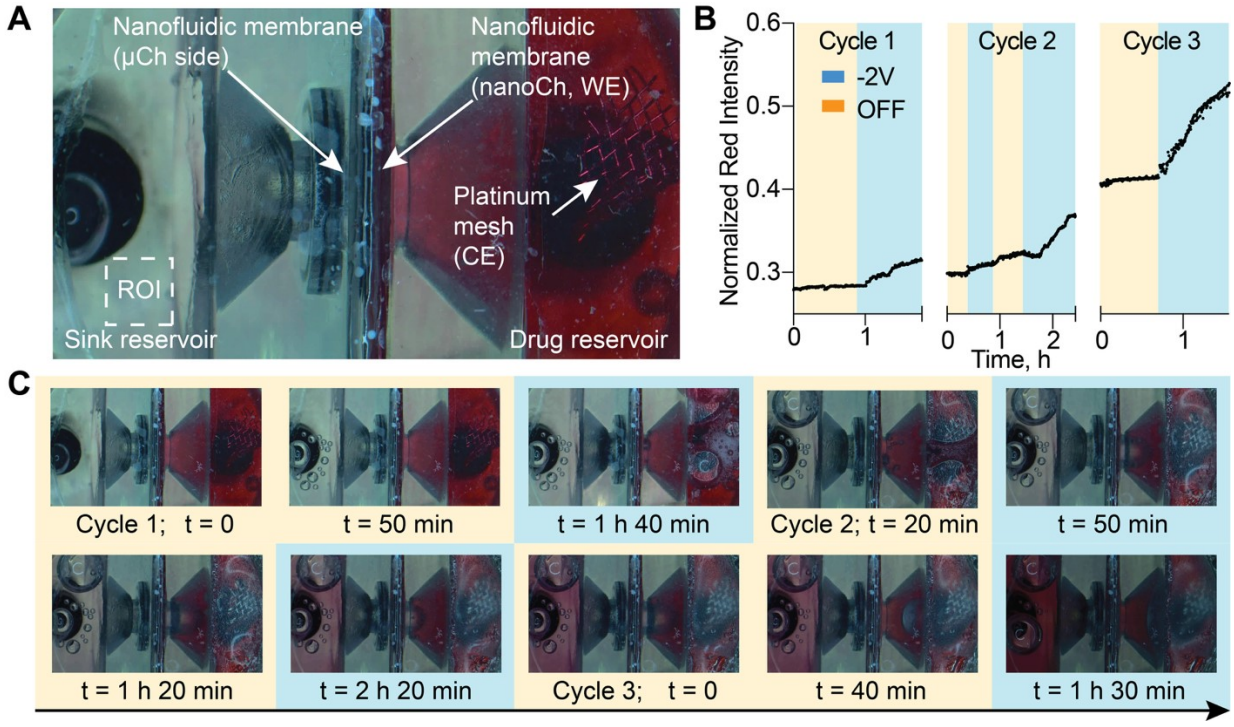

Figure S3. Optical analysis of the electrochemical pump working mechanism. (A) Experimental setup showing the optical imaging configuration at the beginning of the experiment. (B) Normalized red intensity over time and (C) representative time-lapse frames showing bubble formation and convective pumping of VitB12 into the sink reservoir during application of –2 VDC or open-circuit potential (OCP).

Supplementary note 4: *Volume displacement estimation of the electrochemical pump*

The in vitro release modulation data of VitB12 (Fig. 4C) were converted into estimated reservoir volume displacement by correlating the measured mass release rates with the known concentration of VitB12 in the drug reservoir (600 μg/mL). This calculation provides an indirect estimate of the liquid volume displaced from the reservoir during electrochemical actuation. The analysis shows that during active stimulation phases (Phases 1, 3, 5, and 7), the reservoir is displaced at an average rate of approximately 7.16 μL/h (Fig. S4). This representation is useful for visualizing reservoir drainage dynamics during convective pumping through the nanofluidic membrane.

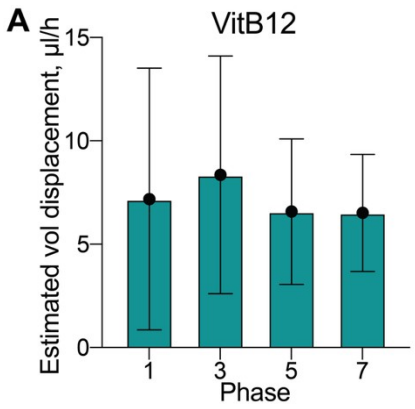

Figure S4. Volume displacement estimation of the electrochemical pump. (A) Estimated volume displacement during –2 VDC actuation, derived from in vitro VitB12 release data. Data highlight the relationship between electrochemical stimulation and reservoir fluid drainage.

Supplementary note 5: *Simulation of dynamic sink conditions*

To evaluate the influence of dynamic sink conditions on drug transport across the nanofluidic membrane, we simulated two continuous flow scenarios—15 mL/day and 50 mL/day—under a constant drug release rate of 4 µg/h into a 30 mL receiving compartment. These flow-based configurations were designed to sustain a consistent concentration gradient between the drug reservoir and the sink compartment, mimicking dynamic clearance mechanisms commonly observed in physiological conditions. For comparison, a static sink condition was modeled using a closed 15 mL volume and the same constant drug release rate, with sink replacement and sampling performed weekly. The simulation underscores the importance of active sink conditions in preserving a high concentration differential across the nanofluidic membrane, thereby supporting physiologically relevant characterization of transport kinetics.

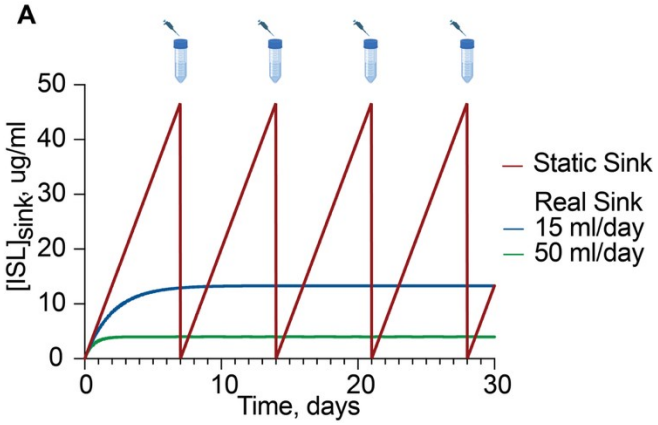

Figure S5. Simulation demonstrating the utility of RSACS. Continuous flow and collection at 15 mL/day and 50 mL/day maintain a stable concentration gradient across the nanofluidic membrane, closely replicating physiological clearance dynamics. In contrast, static conditions

result in drug accumulation, diminishing the driving force for diffusion. The simulation highlights the critical role of dynamic clearance in sustaining effective and consistent drug transport.